ACS Medicinal Chemistry Letters

Letter

Cite This: ACS Med. Chem. Lett. 2017, 8, 1025-1030

pubs.acs.org/acsmedchemlett

Artificial Macrocycles as Potent p53−MDM2 Inhibitors

Natalia Estrada-Ortiz,[†,‡] Constantinos G. Neochoritis,[†,‡] Aleksandra Twarda-Clapa,[#,⊥] Bogdan Musielak,[§] Tad A. Holak,[⊥,§] and Alexander Dömling*[,†]

[†]Department of Drug Design, University of Groningen, A. Deusinglaan 1, Groningen 9700AV, The Netherlands

[#]Faculty of Biochemistry, Biophysics and Biotechnology, Jagiellonian University, Gronostajowa 7, 30-387 Krakow, Poland

[⊥]Malopolska Centre of Biotechnology, Jagiellonian University, Gronostajowa 7a, 30-387 Krakow, Poland

[§]Department of Chemistry, Jagiellonian University, Ingardena 3, 30-060 Krakow, Poland

Supporting Information

ABSTRACT: Based on a combination of an Ugi four component reaction and a ring closing metathesis, a library of novel artificial macrocyclic inhibitors of the p53−MDM2 interaction was designed and synthesized. These macrocycles, alternatively to stapled peptides, target for the first time the large hydrophobic surface area formed by Tyr67, Gln72, His73, Val93, and Lys94 yielding derivatives with affinity to MDM2 in the nanomolar range. Their binding affinity with MDM2 was evaluated using fluorescence polarization (FP) assay and $^{1}H-^{15}N$ two-dimensional HSQC nuclear magnetic resonance experiments.

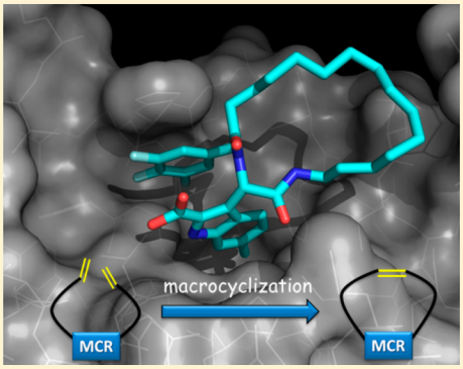

KEYWORDS: *Macrocycles, Ugi reaction, p53, MDM2, protein−protein interaction, cancer*

In nature, macrocycles are not uncommon and often exhibit interesting biological activities.[1] Often macrocyclic compounds have distinct advantages over their open chain analogues including higher affinity and selectivity,[2] preferable entropic signature, better membrane permeation, and oral bioavailability or higher stability.[1,2] Thus, macrocycles can increase affinity and selectivity for a specific target.[1] In spite of their potential, macrocycles pose considerable synthesis problems, and also, the accurate prediction of their conformation makes it difficult to predict activity.[1,2]

The tumor suppressor protein p53 is involved in controlling pathways of cell cycle, apoptosis, angiogenesis metabolism, senescence, and autophagia.[3,4] The TP53 gene is one of the most frequently mutated genes in a multitude of human cancer.[5] Additionally, in multiple cases where TP53 is intact, p53's function is impaired by its negative regulators, mouse double minute 2 and 4 homologues (MDM2 and MDMX), due to amplification or enhanced expression of their coding genes.[3−5] Multiple potent and selective compound classes to inhibit the p53−MDM2 interaction have been discovered, described, and evaluated in early clinical trials.[6] However, the pharmacokinetic and pharmacodynamics properties of the studied scaffolds could still be optimized to minimize the side effects. Thus, the discovery of new p53−MDM2 inhibitors with diverse structures to improve their properties is still of importance.[6−8] The three finger pharmacophore model for p53−MDM2 is recognized as responsible for the binding of small molecules and peptides to the MDM2.[9,10] We already described several series of potent p53−MDM2 antagonists, proposing an extended four finger model; the intrinsically disordered MDM2 *N*-terminus is ordered by certain small molecules, which can be obtained by multicomponent reaction chemistry,[11,12] as shown by cocrystallization.[13,14] Recently, several macrocyclic stapled peptides have been described with great affinity toward MDM2 and MDMX.[6] ALRN-6924 (Aileron Therapeutics) is currently undergoing phase I and II clinical trials in patients suffering from solid tumors, lymphoma, and myeloid leukemias (ClinicalTrials.gov ID: NCT02264613 and NCT02909972).

Here, we propose a novel series of nonpeptidic artificial macrocyclic compounds that inhibit the p53−MDM2 interaction, which might have a different activity profile from the currently available scaffolds. Our synthesis strategy is shown in Figure 1. Based on the Ugi scaffold, we introduced two terminal

Figure 1. Macrocyclization strategy to inhibit the p53−MDM2 interaction.

Received: May 23, 2017
Accepted: September 20, 2017
Published: September 20, 2017

DOI: 10.1021/acsmedchemlett.7b00219
ACS Med. Chem. Lett. 2017, 8, 1025−1030

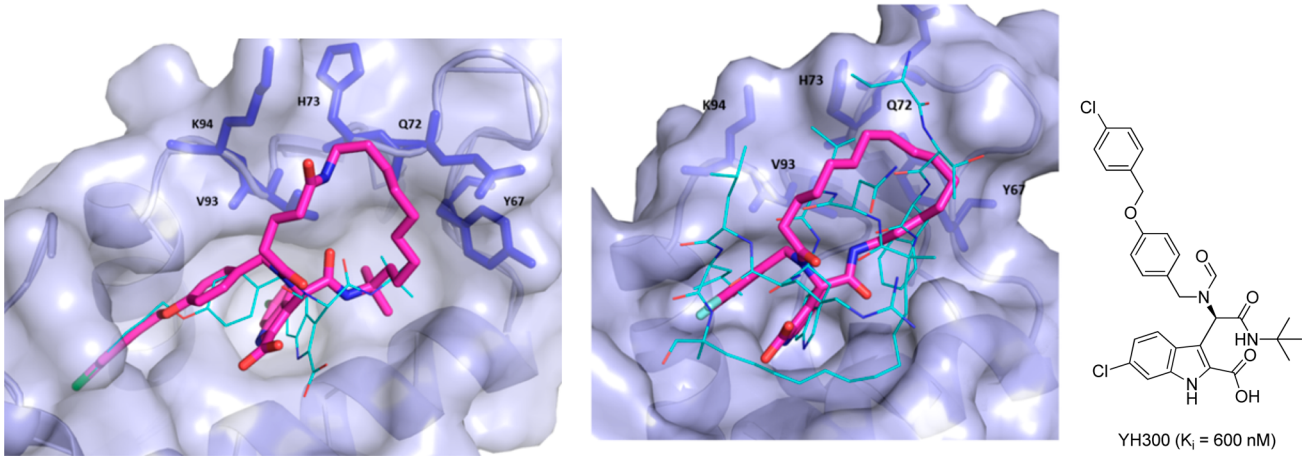

Figure 2. Four- and three-point pharmacophore modeling of macrocyclic compounds. Left: YH300 (PDB ID: 4MDN, cyan lines), Tyr67, Gln72, His73, Val93, and Lys94 (blue sticks), proposed macrocycle to explore the four-pharmacophore point (pink sticks). Right: SAH-p53−8 stapled-peptide (PDB ID: 3V3B, cyan lines), Tyr67, Gln72, His73, Val93, and Lys94 (blue sticks), proposed macrocycle to explore the three-pharmacophore point (pink sticks).

Scheme 1. Retrosynthetic Plan Based on a U-4CR and a Ring Closing Metathesis

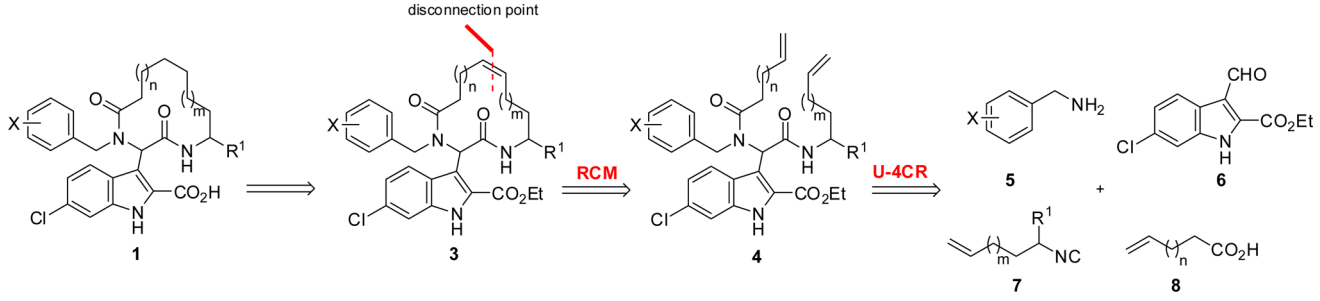

ene-functionalities via the carboxylic acid and the isocyanide component, and we were able to cyclize the compounds by ring closing metathesis (RCM, Figure 1).[15,16]

Our previously introduced three and four-point pharmacophore models were the basis of the discovery and development of the current inhibitors. Thus, we used as the starting point our formerly described α-aminoacylamide (YH300, shown in cyan sticks, Figure 2) with a K_i of 600 nM and its crystal structure in complex with MDM2 receptor (PDB ID 4MDN).[13] Accordingly, the 6-chloroindole-2-carboxylic acid was used as an "anchor" in order to mimic the Trp23 amino acid and constrain the position of other substituents, and three additional binding sites were defined, Phe19, Leu26, and the induced Leu26 subpocket.

Our design of the macrocyclic linker aims to bind on top of the loop linking $\alpha2'$ and $\alpha1'$ helices, covering a large hydrophobic surface area formed by Tyr67, Gln72, His73, Val93, and Lys94 (Figure 2) and potentially increasing the affinity to the receptor. Moreover, we reasoned that the addition of a methyl group on the ring could mimic the *tert*-butyl group of YH300,[13] likely leading to increased affinity.

The retrosynthetic plan of the designed macrocycle **1** foresees (Scheme 1) a ring closing metathesis reaction (RCM), followed by a classical Ugi four-component (U-4CR). The Ugi adduct is formed of the anchoring 6-chloro-3-carboxaldehyde **6**, suitably substituted benzylamines **5**, and the long-chained aliphatic carboxylic acids **8** along with the isocyanides **7** incorporating terminal double bonds.

Aldehyde **6** was synthesized from the 6-chloro-indole derivative using the Vilsmeier−Haack formylation reaction.[17,18]

For the preliminary structure−activity relationship (SAR) analysis of the Leu26 and the induced pockets, the benzylamines **5** were used as commercially available (**5b−h**) or obtained via Williamson ether synthesis (**5a**). Probing both the Phe19 pocket and the larger hydrophobic surface area formed by Tyr67, Gln72, His73, Val93, and Lys94, the isocyanides **7a,b** were synthesized from the corresponding formamides, whereas the carboxylic acids are commercially available. In particular, the amine **5a** with the oxygen linker that was designed to probe the induced pocket was synthesized through a Williamson ether synthesis of the protected 4-hydroxybenzylamine with the 3,4-benzyl chloride under basic conditions (Supporting Information (SI), Scheme 1). The isocyanides **7a,b** were synthesized from the formamides via the revised Leuckart−Wallach reaction of the corresponding carbonyl compounds (SI, Scheme 2).[19]

Next, we proceeded in the Ugi four-component reaction. Equimolar mixture of the substituted benzylamine **5**, aldehyde **6**, isocyanide **7**, and carboxylic acid **8** in 2,2,2-trifluoroethanol (TFE) was irradiated at 120 °C for 1 h in a microwave oven yielding compounds **4** (Scheme 2). Afterward, we successfully performed the ring closing metathesis with the second generation of Grubbs catalyst in dichloromethane (DCM) affording compounds **3** as mixture of isomers (*E* and *Z*). Due to the fact that the existence of the double bond gives rise to two possible isomers and most importantly reduces the flexibility of the macrocycle, we decided to subject the mixture to hydrogenation on Pd/C isolating compounds **2**. The last step was the ester hydrolysis obtaining the final screening compounds **1** (Scheme 2). Performing a preliminary SAR, we built a small

DOI: 10.1021/acsmedchemlett.7b00219
ACS Med. Chem. Lett. 2017, 8, 1025−1030

Scheme 2. Synthesis of the Macrocycle Library Based on the U-4CR/RCM Strategy

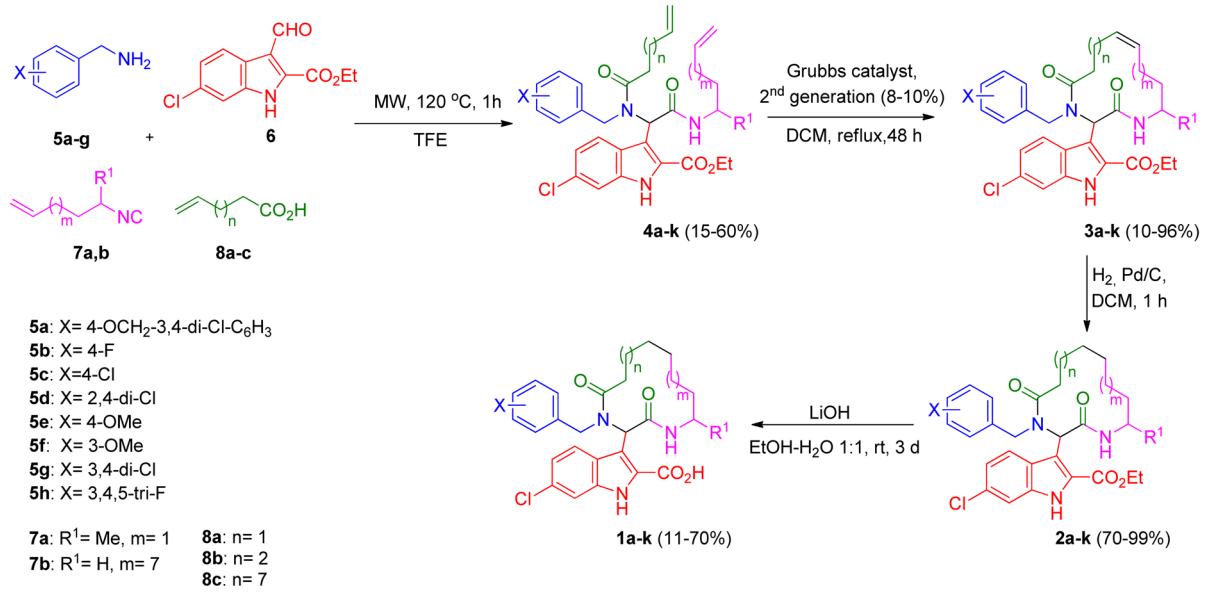

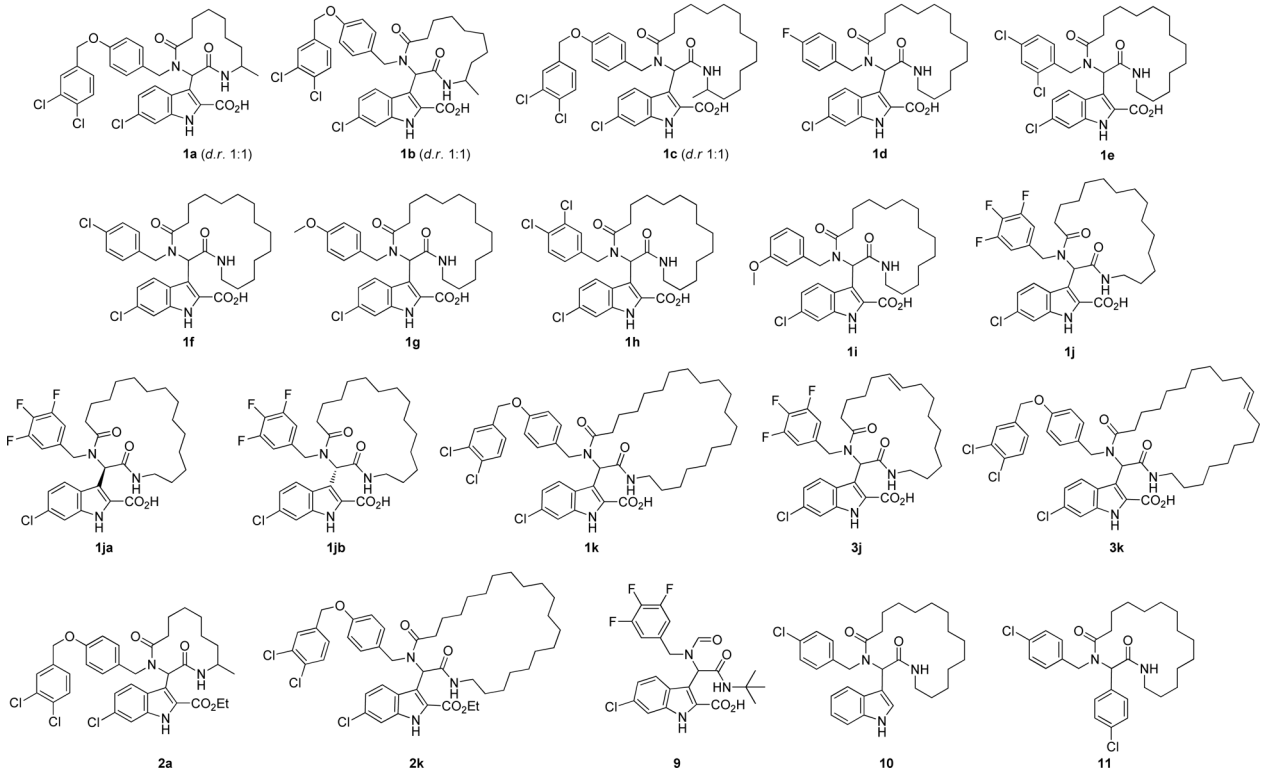

library of macrocycles of various ring sizes (12, 13, 18, 19, and 24 number of atoms) targeting the hydrophobic region around Tyr67, Gln72, His73, Val93, and Lys94. We maintained the anchoring indole group for the Trp23 and the phenyl group for Leu26 and further explored the induced pocket with the extended dichlorobenzyloxy moiety.

Two complementary assays based on independent physicochemical principles, fluorescence polarization (FP) and $^{1}H-^{15}N$ 2D HSQC nuclear magnetic resonance (NMR) were used to measure affinity and to exclude false positive hits. FP assay was employed to determine the inhibitory affinities (K_i) of the macrocycles against MDM2 as previously described,[20] and the results are presented in Table 1.

Examining both the three- and four-finger pharmacophore model, it seems that most of the obtained macrocycles are active toward MDM2, many of them demonstrating an affinity below 1 μM. Although it is a preliminary SAR study, we can conclude that the ideal ring size for the four-finger model seems to be around 18 (entry 3). The affinity improves while increasing the size from 12 (**1a**, entry 1) to 13 (**1b**, entry 2) and eventually 18 (**1c**, entry 3) atom ring size. Moreover, compound **1c** has an affinity of 100 nM as a mixture of diastereomers, whereas the larger 24-membered macrocycle **1k** (entry 11) shows decreased activity (1.91 μM).

In addition, we focused on the three-finger-pharmacophore model, which characterizes the vast majority of the currently

DOI: 10.1021/acsmedchemlett.7b00219
ACS Med. Chem. Lett. 2017, 8, 1025−1030

Table 1. Results of the Evaluation of Inhibitory Activity of Macrocyclic Inhibitors toward MDM2 Using FP Assay[a]

entry	compound	ring size	K_i (μM)
1	**1a**	12	0.35
2	**1b**	13	0.32
3	**1c**	18	0.10
4	**1d**	18	N/A
5	**1e**	18	5.3
6	**1f**	18	N/A
7	**1g**	18	1.3
8	**1h**	18	0.08
9	**1i**	18	1.8
10	**1j**	19	0.14 (*rac*-**1j**) 0.09 {(+)-**1ja**} 0.70 {(−)-**1jb**}
11	**1k**	24	1.9
12	**3j**	19	0.34
13	**3k**	24	2.5
14	**2a**	12	3.0
15	**2k**	24	N/A

[a]N/A: not active; all measurements performed in duplicates; standard errors up to 10%.

available small-molecule MDM2 inhibitors.[6] We synthesized various macrocycles with a different substitution pattern. The position of halogens on the phenyl group seems to play a significant role since the *para* fluoro (**1d**, entry 4) or chloro substituted (**1f**, entry 6) derivatives are only slightly or not active at all. On the contrary, the addition of a second chlorine in *o*- or *m*-position influenced the binding mode, the 2,4-dichloro derivative (**1e**) showed activity of 5.3 μM (entry 5,) and the corresponding 3,4-dichloro compound **1h** (entry 8) displayed an activity of 80 nM. Whereas placing the donor group −OMe in compound **1g** (entry 7) improved the affinity with 1.3 μM. Nonetheless, *m*-OMe substitution, keeping the same ring size of 18 (**1i**, entry 9), did not show any significant difference, exhibiting an activity of 1.8 μM. Due to our previous results,[21] where we were able to synthesize fluorinated phenyls such as compound **9** with K_i up to 100 nM, we employed the 3,4,5-trifluorobenzylamine and we synthesized compound **1j** (entry 10), which exhibited an interesting affinity as a racemic mixture of 140 nM. Enantiomeric separation of the racemic mixture via chiral SFC provided the enantiomers (+)-**1ja** and (−)-**1jb** with affinities of 90 and 700 nM, respectively. As it was expected, the separated enantiomers showed a significant increase of the activity compared to the racemic mixture.

The existence of the double bond in the macrocycles **3j** and **3k**, as anticipated, reduced significantly the affinity to 340 nM and 2.5 μM, respectively (entries 12 and 13), compared with the corresponding hydrogenated compounds **1j** (K_i = 140 nM) and **1k** (K_i = 1.9 μM). The corresponding esters, **2a** and **2k** (entries 14 and 15), are orders of magnitude less reactive or inactive comparing with the acids in accordance with our previous experience (entries 1 and 11).[11,12,22−25] Interestingly, the acyclic Ugi-adduct **4j** was also proven to be practically inactive both in the ester and acid forms (SI, Table S1, entry 15). Moreover, changing the anchor to a nonsubstituted indole moiety (compound **10**) or to the 3- or 4-phenyl moiety (compound **11**), resulted in nearly no activity.

The expected ligand-induced perturbations in $^{1}H-^{15}N$ 2D HSQC NMR spectra were indeed observed (Figure 3). The ^{15}N-labeled MDM2 was titrated with increasing concentration of the

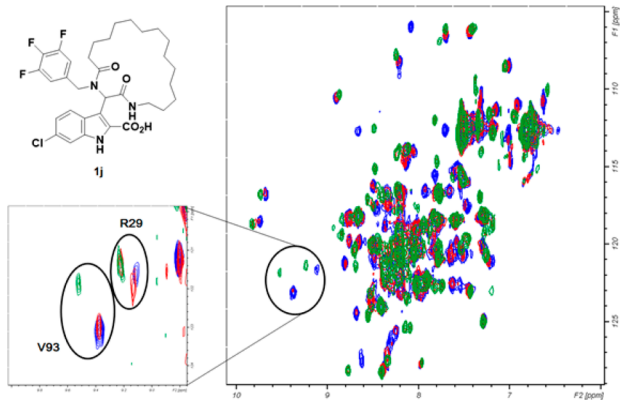

Figure 3. Spectrum of the ^{15}N-labeled MDM2 (blue) superimposed with spectrum after addition of **1j** in a MDM2/**1j** molar ratio equal to 2:1 (red) and 1:1 (green). The close-up view shows selected peaks assigned to Val93 and Arg29. For Arg29, NMR signal splitting indicates strong interaction at K_d below 1 μM.

compound. Since all cross peaks in the MDM2 spectrum were assigned to particular amino acid residues,[26] it was possible to analyze the interaction within the MDM2/**1j** complex. Particularly, Val93 is clearly involved in the interaction, as its cross peak shifted between titration steps for MDM2/**1j** molar ratios equal to 2:1 and 1:1. After 1:1 step, the peak remained in the same position. NMR titration also confirmed the tight binding of **1j**, as, e.g., for Arg29, NMR signal splitting was observed (Figure 3), which indicated strong interaction with MDM2 at K_d below 1 μM (and a slow chemical exchange).

Three of the macrocyclic compounds (**1c**, **1h**, and **1j**) obtained demonstrated improved binding affinities ($K_i \approx$ 100 nM) over the lead acyclic molecule, YH300 (K_i = 600 nM). In order to rationalize the tight receptor ligand interaction, we exploit modeling studies using MOLOC[27] based on the HSQC binding data having as template a known cocrystal structure (PDB ID: 3TU1)[21] and the small network analysis using Scorpion software (Figure 4).[28] It revealed the existence of van der Waals interactions of the aliphatic handle with Tyr67 and His73, the expected alignment of the 6-chloro-indole moiety of the designed compounds with the ^{p53}Trp23 pocket, whereas the

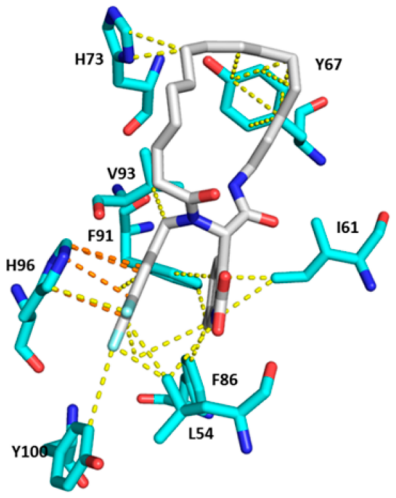

Figure 4. Small network analysis of **1j** (white sticks) modeled into the MDM2 receptor (PDB ID: 3TU1, cyan sticks): $\pi-\pi$ and van der Waals interactions are shown in orange and yellow dotted lines, respectively.

DOI: 10.1021/acsmedchemlett.7b00219
ACS Med. Chem. Lett. 2017, 8, 1025−1030

3,4,5-trifluorophenyl ring occupied the ^{P53}Leu26 hydrophobic pocket. Moreover, the $\pi-\pi$ interaction of His96 with the 3,4,5-trifluorophenyl fragment and several van der Waals interactions with Leu54, Ile61, Phe86, Phe91, Val93, His96, and Tyr100 are depicted. These findings support our initial hypothesis of the divergent hydrophobic handle position compared to staple peptides shown before,[29−34] suggesting a new approach to improve and diversify the extensive collection of MDM2/X inhibitors.

To analyze and compare the physicochemical properties of our newly synthesized macrocycles with the orally available macrocycle drugs,[35] we plotted molecular weight, clogP, topological polar surface area (TPSA), number of hydrogen bond donors (HBDs), hydrogen bond acceptors (HBAs), and number of rotatable bonds (RB) (Figure 5). Interestingly, the values of the

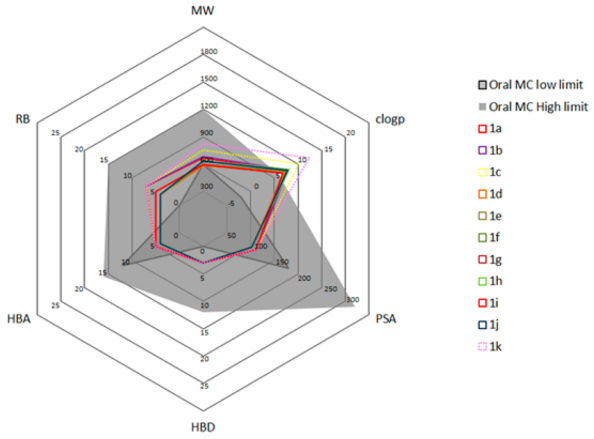

Figure 5. Physicochemical properties of the synthesized macrocycles, compared with the oral macrocycle marketed drugs on a hexagon radar graph. The dark gray area contains the low limits of the oral macrocycle drugs, whereas the light gray shows the highest limits.

properties in most of our macrocycles are set in the appropriate range, demonstrating the significance of this new strategy to develop potentially oral bioavailable macrocycles targeting the p53−MDM2 interaction. In the case of **1c** and **1k**, clogP goes off the limits as expected since we were targeting a very lipophilic surface. However, this will be overcome in the future with a strategy to incorporate heteroatoms (oxygens) on both the acid and isocyanide linker. After this initial SAR study, we will in the future synthesize libraries of novel macrocycles as potent p53−MDM2 inhibitors with higher diversity and complexity.

■ ASSOCIATED CONTENT

Supporting Information

The Supporting Information is available free of charge on the ACS Publications website at DOI: 10.1021/acsmedchemlett.7b00219.

General procedures, characterization data, and screening results exemplary copies of NMR (PDF)

■ AUTHOR INFORMATION

Corresponding Author

*Tel: +31503633307. Fax: +31503637582. E-mail: a.s.s.domling@rug.nl.

ORCID

Constantinos G. Neochoritis: 0000-0001-5098-5504

Tad A. Holak: 0000-0001-9369-6024

Alexander Dömling: 0000-0002-9923-8873

Author Contributions

‡These authors contributed equally. The manuscript was written through contributions of all authors. All authors have given approval to the final version of the manuscript.

Funding

Research in the area of p53−MDM2/X interactions in the Dömling research group was supported by the US National Institutes of Health (NIH) (2R01GM097082-05). Funding has been received from the European Union's Horizon 2020 research and innovation program under MSC ITN "Accelerated Early stage drug dIScovery" (AEGIS, grant agreement No. 675555) and CoFund ALERT (grant agreement No. 665250). N.E.O. was supported by the Department of Sciences, Technology, and Innovation-COLCIENCIAS (Colombia).

Notes

The authors declare no competing financial interest.

■ REFERENCES

(1) Driggers, E. M.; Hale, S. P.; Lee, J.; Terrett, N. K. The Exploration of Macrocycles for Drug Discovery-An Underexploited Structural Class. *Nat. Rev. Drug Discovery* **2008**, *7* (7), 608−624.

(2) Giordanetto, F.; Kihlberg, J. Macrocyclic Drugs and Clinical Candidates: What Can Medicinal Chemists Learn from Their Properties? *J. Med. Chem.* **2014**, *57* (2), 278−295.

(3) Lane, D. P. p53, Guardian of the Genome. *Nature* **1992**, *358* (6381), 15−16.

(4) Klein, C.; Vassilev, L. T. Targeting the p53−MDM2 Interaction to Treat Cancer. *Br. J. Cancer* **2004**, *91* (8), 1415−1419.

(5) Vogelstein, B.; Lane, D.; Levine, A. J. Surfing the p53 Network. *Nature* **2000**, *408* (6810), 307−310.

(6) Estrada-Ortiz, N.; Neochoritis, C. G.; Dömling, A. How To Design a Successful p53−MDM2/X Interaction Inhibitor: A Thorough Overview Based on Crystal Structures. *ChemMedChem* **2016**, *11* (8), 757−772.

(7) Khoo, K. H.; Verma, C. S.; Lane, D. P. Drugging the p53 Pathway: Understanding the Route to Clinical Efficacy. *Nat. Rev. Drug Discovery* **2014**, *13* (3), 217−236.

(8) Zhao, Y.; Aguilar, A.; Bernard, D.; Wang, S. Small-Molecule Inhibitors of the MDM2−p53 Protein−Protein Interaction (MDM2 Inhibitors) in Clinical Trials for Cancer Treatment. *J. Med. Chem.* **2015**, *58* (3), 1038−1052.

(9) Chen, J.; Marechal, V.; Levine, A. J. Mapping of the p53 and Mdm-2 Interaction Domains. *Mol. Cell. Biol.* **1993**, *13* (7), 4107−4114.

(10) Picksley, S. M.; Vojtesek, B.; Sparks, A.; Lane, D. P. Immunochemical Analysis of the Interaction of p53 with MDM2; Fine Mapping of the MDM2 Binding Site on p53 Using Synthetic Peptides. *Oncogene* **1994**, *9* (9), 2523−2529.

(11) Shaabani, S.; Neochoritis, C. G.; Twarda-Clapa, A.; Musielak, B.; Holak, T. A.; Dömling, A. Scaffold Hopping via ANCHOR.QUERY: β-Lactams as Potent p53−MDM2 Antagonists. *MedChemComm* **2017**, *8*, 1046−1052.

(12) Surmiak, E.; Neochoritis, C. G.; Musielak, B.; Twarda-Clapa, A.; Kurpiewska, K.; Dubin, G.; Camacho, C.; Holak, T. A.; Dömling, A. Rational Design and Synthesis of 1,5-Disubstituted Tetrazoles as Potent Inhibitors of the MDM2-p53 Interaction. *Eur. J. Med. Chem.* **2017**, *126*, 384−407.

(13) Bista, M.; Wolf, S.; Khoury, K.; Kowalska, K.; Huang, Y.; Wrona, E.; Arciniega, M.; Popowicz, G. M.; Holak, T. A.; Dömling, A. Transient Protein States in Designing Inhibitors of the MDM2-p53 Interaction. *Structure* **2013**, *21* (12), 2143−2151.

(14) Bauer, M. R.; Boeckler, F. M. Hitting a Moving Target: Targeting Transient Protein States. *Structure* **2013**, *21* (12), 2095−2097.

(15) Beck, B.; Larbig, G.; Mejat, B.; Magnin-Lachaux, M.; Picard, A.; Herdtweck, E.; Dömling, A. Short and Diverse Route toward Complex Natural Product-like Macrocycles. *Org. Lett.* **2003**, *5* (7), 1047−1050.

DOI: 10.1021/acsmedchemlett.7b00219
ACS Med. Chem. Lett. 2017, 8, 1025−1030

(16) Wessjohann, L. A.; Rivera, D. G.; Vercillo, O. E. Multiple Multicomponent Macrocyclizations (MiBs): A Strategic Development toward Macrocycle Diversity. *Chem. Rev.* **2009**, *109* (2), 796−814.
(17) Dömling, A. P53-mdm2 Antagonists. Patent Application WO 2012/033525 A3, 2012.
(18) Dömling, A.; Holak, T. Novel p53-mdm2/p53-mdm4 Antagonists to Treat Proliferative Disease. Patent application WO2011106650 A3, 2012.
(19) Neochoritis, C. G.; Zarganes-Tzitzikas, T.; Stotani, S.; Dömling, A.; Herdtweck, E.; Khoury, K.; Dömling, A. Leuckart−Wallach Route Toward Isocyanides and Some Applications. *ACS Comb. Sci.* **2015**, *17* (9), 493−499.
(20) Czarna, A.; Popowicz, G. M.; Pecak, A.; Wolf, S.; Dubin, G.; Holak, T. A. High Affinity Interaction of the p53 Peptide-Analogue with Human Mdm2 and Mdmx. *Cell Cycle* **2009**, *8* (8), 1176−1184.
(21) Huang, Y.; Wolf, S.; Koes, D.; Popowicz, G. M.; Camacho, C. J.; Holak, T. A.; Dömling, A. Exhaustive Fluorine Scanning toward Potent p53−Mdm2 Antagonists. *ChemMedChem* **2012**, *7* (1), 49−52.
(22) Neochoritis, C. G.; Wang, K.; Estrada-Ortiz, N.; Herdtweck, E.; Kubica, K.; Twarda, A.; Zak, K. M.; Holak, T. A.; Dömling, A. 2,3′-Bis(1′H-Indole) Heterocycles: New p53/MDM2/MDMX Antagonists. *Bioorg. Med. Chem. Lett.* **2015**, *25* (24), 5661−5666.
(23) Czarna, A.; Beck, B.; Srivastava, S.; Popowicz, G. M.; Wolf, S.; Huang, Y.; Bista, M.; Holak, T. A.; Dömling, A. Robust Generation of Lead Compounds for Protein-Protein Interactions by Computational and MCR Chemistry: p53/Hdm2 Antagonists. *Angew. Chem., Int. Ed.* **2010**, *49* (31), 5352−5356.
(24) Huang, Y.; Wolf, S.; Bista, M.; Meireles, L.; Camacho, C.; Holak, T. A.; Dömling, A. 1,4-Thienodiazepine-2,5-Diones via MCR (I): Synthesis, Virtual Space and p53-Mdm2 Activity. *Chem. Biol. Drug Des.* **2010**, *76* (2), 116−129.
(25) Srivastava, S.; Beck, B.; Wang, W.; Czarna, A.; Holak, T. A.; Dömling, A. Rapid and Efficient Hydrophilicity Tuning of p53/mdm2 Antagonists. *J. Comb. Chem.* **2009**, *11* (4), 631−639.
(26) Rehm, T.; Huber, R.; Holak, T. A. Application of NMR in Structural Proteomics: Screening for Proteins Amenable to Structural Analysis. *Structure* **2002**, *10* (12), 1613−1618.
(27) Gerber, P. R.; Müller, K. MAB, a Generally Applicable Molecular Force Field for Structure Modelling in Medicinal Chemistry. *J. Comput.-Aided Mol. Des.* **1995**, *9* (3), 251−268.
(28) Kuhn, B.; Fuchs, J. E.; Reutlinger, M.; Stahl, M.; Taylor, N. R. Rationalizing Tight Ligand Binding through Cooperative Interaction Networks. *J. Chem. Inf. Model.* **2011**, *51* (12), 3180−3198.
(29) Phan, J.; Li, Z.; Kasprzak, A.; Li, B.; Sebti, S.; Guida, W.; Schönbrunn, E.; Chen, J. Structure-Based Design of High Affinity Peptides Inhibiting the Interaction of p53 with MDM2 and MDMX. *J. Biol. Chem.* **2010**, *285* (3), 2174−2183.
(30) Baek, S.; Kutchukian, P. S.; Verdine, G. L.; Huber, R.; Holak, T. A.; Lee, K. W.; Popowicz, G. M. Structure of the Stapled p53 Peptide Bound to Mdm2. *J. Am. Chem. Soc.* **2012**, *134* (1), 103−106.
(31) Pazgier, M.; Liu, M.; Zou, G.; Yuan, W.; Li, C.; Li, C.; Li, J.; Monbo, J.; Zella, D.; Tarasov, S. G.; Lu, W. Structural Basis for High-Affinity Peptide Inhibition of p53 Interactions with MDM2 and MDMX. *Proc. Natl. Acad. Sci. U. S. A.* **2009**, *106* (12), 4665−4670.
(32) Zhan, C.; Zhao, L.; Wei, X.; Wu, X.; Chen, X.; Yuan, W.; Lu, W.-Y.; Pazgier, M.; Lu, W. An Ultrahigh Affinity D-Peptide Antagonist Of MDM2. *J. Med. Chem.* **2012**, *55* (13), 6237−6241.
(33) Liu, M.; Li, C.; Pazgier, M.; Li, C.; Mao, Y.; Lv, Y.; Gu, B.; Wei, G.; Yuan, W.; Zhan, C.; Lu, W.-Y.; Lu, W. D-Peptide Inhibitors of the p53−MDM2 Interaction for Targeted Molecular Therapy of Malignant Neoplasms. *Proc. Natl. Acad. Sci. U. S. A.* **2010**, *107* (32), 14321−14326.
(34) Chee, S. M. Q.; Wongsantichon, J.; Soo Tng, Q.; Robinson, R.; Joseph, T. L.; Verma, C.; Lane, D. P.; Brown, C. J.; Ghadessy, F. J. Structure of a Stapled Peptide Antagonist Bound to Nutlin-Resistant Mdm2. *PLoS One* **2014**, *9* (8), e104914.
(35) Villar, E. A.; Beglov, D.; Chennamadhavuni, S.; Porco, J. A.; Kozakov, D.; Vajda, S.; Whitty, A. How Proteins Bind Macrocycles. *Nat. Chem. Biol.* **2014**, *10* (9), 723−731.

DOI: 10.1021/acsmedchemlett.7b00219
ACS Med. Chem. Lett. 2017, 8, 1025−1030